Paper Jurnal/Prosiding

by I Putu Dody Lesmana

Submission date: 01-May-2023 04:48PM (UTC+0700)
Submission ID: 2080785477
File name: Prosiding.pdf (454.07K)
Word count: 4308
Character count: 22261

2011 International Conference on Instrumentation, Communication, Information Technology and Biomedical Engineering
8-9 November 2011, Bandung, Indonesia

Abnormal Condition Detection of Pancreatic Beta-Cells as the Cause of Diabetes Mellitus Based on Iris Image

I Putu Dody Lesmana[1] I Ketut Eddy Purnama[2] Mauridhi Hery Purnomo[2]
[1]Department of Information Technology, Polytechnic State of Jember, PO Box 164, Jember, Indonesia
E-mail: dody@polije.ac.id
[2]Department of Electrical Engineering, Faculty of Industrial Technology ITS, 60111, Surabaya, Indonesia
E-mail: {ketut,hery}@ee.its.ac.id

Abstract- Diabetes occurs due to destruction of Beta-cells in the pancreatic islets of Langerhans with resulting loss of insulin production. The result of insufficient action of insulin is an increase in blood glucose concentration. The diagnosis of Diabetes must always be established by a blood glucose measurement made in an accredited laboratory. The alternative way to measure a deficiency of insulin from the Beta-cells of pancreatic islets uses iris diagnosis. Evaluating the iris is done by detecting the presence of some broken tissue in iris. However, conventional iris diagnosis is always concerned with the identification of syndromes rather than with the connection between abnormal iris tissue appearances and diseases. In this paper, we present a novel computerized iris inspection method aiming to address these problems for detecting insulin deficiency from the Beta-cells of pancreatic islets. First, quantitative features, textural measures are extracted from iris images by using popular digital image processing techniques. Then, Neighborhood based Modified Backpropagation using Adaptive Learning Parameters (ANMBP) method is employed to model the relationship between quantitative features and pancreatic abnormalities as caused of insulin deficiency. The effectiveness of this method is tested on 12 patients with Diabetes, and the diagnostic results predicted by the previously trained ANMBP classifiers are compared with the calculation of HOMA-B, obtained 83.3% accuracy in detecting pancreas disorders.

Keyword: Computerized iris diagnosis, texture, ANMBP, neighborhood, HOMA-B.

I. INTRODUCTION

Diabetes Mellitus (DM) is due to destruction of Beta-cells in the pancreatic islets of Langerhans with resulting insulin deficiency. The result of insufficient action of insulin is an increase in blood glucose concentration (hyperglycemia). Many other metabolic abnormalities occur, notably an increase in ketone bodies in the blood when there is a severe lack of insulin. Thirst, tiredness, pruritus vulvae or balanitis, polyuria, and weight loss are the familiar symptoms of DM. But the diagnosis of DM is so often missed because of patients do not, of course, always describe their symptoms in the clearest possible terms, or else their complaints may occur only as an indirect consequence of the more common features. Many patients describe dry mouth rather than thirst, and patients have been investigated for dysphagia when dehydration was the cause. Polyuria may cause enuresis in young people and incontinence in elderly people and the true diagnosis is often overlooked.

To prevent diagnosis of DM should no longer be missed; new patients should have a blood glucose measurement as a matter of routine, especially if their symptoms are unexplained. According to Jensen [1], we evaluate alternative method to diagnose DM based on iris image that is called iris diagnosis. Iris diagnosis is one of the most valuable and widely used diagnostic methods along with other diagnostic techniques to facilitate a more complete understanding of their patient health care needs. As iris diagnosis has played such a prominent role in the diagnosis and the subsequent treatment of diseases, it has attracted an increasing amount of attention both in clinical medicine and in biomedicine. However, iris diagnosis has inevitable limitations that impede its medical applications. First, the clinical competence of iris diagnosis is determined by the experience and knowledge of the practitioners. Second, iris diagnosis is usually based on the detailed visual discrimination by learning the formation of tissues in iris. Therefore, it depends on the subjective analysis of the practitioners, so that the diagnostic results may be unreliable and inconsistent. Finally, conventional iris diagnosis is intimately related to the identification of syndromes (also called patterns), and it is not very well understood in Western medicine and modern biomedicine. Therefore, it is necessary to build an objective and quantitative diagnostic standard for iris diagnosis, and explore the relations between features and diseases.

Recently, researchers have been developing various methods and systems [2]–[4] to circumvent these problems. Despite considerable progress in the standardization and quantification of iris diagnosis, there are significant problems with the existing approaches. First, some methods do not describe the preparation of protocols for medical data retrieval. This must be met for the proposed method can be accepted by the clinical medicine and tested to meet the eligibility of medical ethics. Second, many of the developed models are only dedicated to the recognition of pathological features defined in conventional iris diagnosis, and the mapping from images of the iris to

978-1-4577-1166-4/11/$26.00 ©2011 IEEE

diseases is not considered. This will undoubtedly limit the applications of these approaches in clinical medicine.

In this paper, we propose a computerized iris diagnosis method based on quantitative features and a training algorithm using Modified Backpropagation algorithm [5] in neighborhood based network structure [6] by replacing fixed learning parameters with adaptive learning parameters [7] called ANMBP [8] for the diagnosis of the condition of pancreas organ as the cause of DM. The outline of a computerized iris diagnosis system that uses a ANMBP network as the feature-matching model is illustrated in Fig. 1. Our method is dedicated to the feature extraction and matching processes.

II. Iris Diagnosis Using ANMBP

Normally, standard Backpropagation (BP) algorithm for feed forward neural network (FNN) learning are based on gradient descent method [9,10]. But the algorithm is too slow and stuck in local minima. Many fast learning algorithms were proposed based on the application of different optimization techniques and the adaptation of learning rate and momentum rate in the conventional BP algorithm.

Abid et al. [5] described Modified BP (MBP) algorithm based on sum of linear and non linear errors of output neurons to improve the speed of convergence in minimum iterations. The algorithm converges faster than the standard BP algorithm for an appropriate choice of learning rate λ. Here choice of λ is very difficult. Because small value of λ does not influence convergence speed and high value cause divergence of algorithm [5]. To have better convergence speed and to avoid local minima to some extent, fixed learning parameters could be replaced by adaptive learning parameters [7]. Behera et al. [7] have described new learning algorithm LFII based on Lyapunov function for the training of FNN by using adaptive learning rate and adaptive acceleration term. The algorithm improves the convergence speed and escapes from local minima. Lera and Pinzolas [6] have developed the neighborhood based LM method (NBLM) to improve the algorithm in both time and memory. An optimization in a reduced subspace of the weight space at each iteration is performed in their work. Pinzolas et al. [6] have described neighborhood based training method which improves the method efficiently by reducing memory and time.

In proposed a training algorithm (ANMBP), we summarize the existing improved algorithms [5]–[8] , to have better convergence speed and avoid local minima to some extent. As for computerized iris diagnosis, there is a point should be mentioned when using a ANMBP as a diagnostic model. The point concerning the use of a ANMBP as a diagnostic model is that, all of the input nodes in our model represent quantitative textural features obtained by using image processing techniques, which are not directly related to qualitative pathological features employed in conventional iris diagnosis. This is consistent with the original intention of our method: the quantification and objectification of conventional iris diagnosis.

A. Network Structure

ANMBP divide network into different neighborhoods. The main idea is to consider these neighborhoods as independent learning units. Although any set of weights can be considered as a neighborhood, it seems reasonable to select those containing neurons from all the layers and including all the weights belonging to those neurons. Otherwise, there could be some neighborhoods that group unrelated sets of neurons or that are not connected to the inputs or the outputs. With these types of neighborhoods, there is always some overlapping among those that share some output neuron. A typical neighborhood of the kind considered in this work is depicted in Fig. 2. In Fig. 2, N10-12-6–1 represents neighborhood structure with 10 input neurons, 12 and 6 hidden neurons in the neighborhoods and one output neuron. We have studied both the effect of the size and overlapping of the neighborhoods. Operation of biological neural networks suggests that overlapping should be important, but in the performed experiments, there is almost no difference between overlapping and isolated neighborhoods (except for the output neuron). The set of neighborhoods was selected at random before training, and in the learning phase, they were sequentially trained.

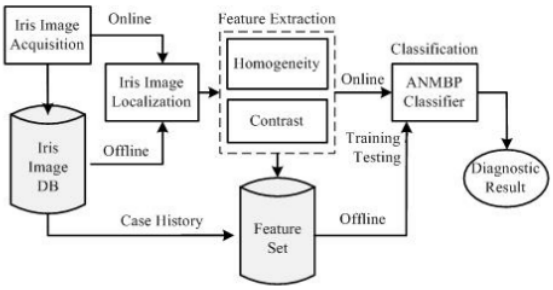

Fig. 1. The outline of the computerized iris diagnosis system.

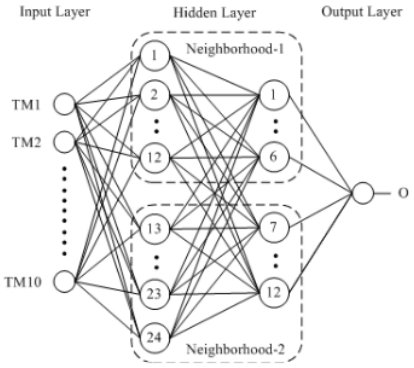

Fig. 2. Neuron neighborhood with N10-12-6-1 structure.

B. Algorithm

In this proposed method, first define the neighborhood and assign value for μ and λ in (5) and (6) as per Behera et al. [7]. One neighborhood is selected randomly and the output and corresponding errors of FNN are calculated for selected pattern. Weights of output and hidden layer neurons corresponding to that neighborhood are updated using (7) by calculating adaptive learning parameters. This training process is repeated for all input patterns. Then the error of the network is calculated. The above procedure to be repeated until desired accuracy is obtained.

Step 1. Initialization.
Define network structure, assign initial weights randomly and define neighborhoods.
Step 2. Select a neighborhood randomly.
Step 3. Select a training pattern.
Select a pattern to be processed into the network.
Step 4. For each node in the hidden layer, compute
Net value using Eq. (1).

$$u_j^{[s]} = b_j^{[s]} + \sum_{i=0}^{n_{s-1}} w_{ji}^{[s]} y_i^{[s-1]} \tag{1}$$

Outputs value using Eq. (2).

$$f\left(u_j^{[s]}\right) = \frac{1}{1+e^{-u_j^{[s]}}} = y_j^{[s]} \tag{2}$$

where jth is neuron in any given layer s.
Step 5. For the output layer, compute
Net value using (1) and output value using (2).
Nonlinear and linear errors using (3) and (4).

$$e_{1_j}^{[s]} = d_j^{[s]} - y_j^{[s]} \tag{3}$$

$$e_{2_j}^{[s]} = f^{-1}\left(d_j^{[s]}\right) - u_j^{[s]} \tag{4}$$

where $d_j^{[s]}$ and $y_j^{[s]}$ are desired and current output for jth unit in the sth layer. Change of weight using (5), (6) and (7) for the selected neighborhood only.

$$\eta_a^{'} = \frac{\mu \left\| e_{1_j}^{[s]} \right\|^2}{\left\| f'\left(u_j^{[s]}\right) y_i^{[s-1]} e_{1_j}^{[s]} \right\|^2 + \varepsilon} \tag{5}$$

$$\mu_a^{'} = \frac{\lambda}{\left\| f'\left(u_j^{[s]}\right) y_i^{[s-1]} e_{1_j}^{[s]} \right\|^2 + \varepsilon} \tag{6}$$

$$\Delta w_{ji}^{[s]} = \eta_a^{'} y_i^{[s-1]} f'\left(u_j^{[s]}\right) e_{1_j}^{[s]} + \mu_a^{'} y_i^{[s-1]} e_{2_j}^{[s]} \tag{7}$$

Step 6. For the hidden layer, compute
Nonlinear estimation error using Eq. (8).

$$e_{1_j}^{[s]} = \sum_{r=1}^{n_{s+1}} e_{1_r}^{[s+1]} f'\left(u_r^{[s+1]}\right) w_{rj}^{[s+1]} \tag{8}$$

Linear error using Eq. (9).

$$e_{2_j}^{[s]} = f'\left(u_j^{[s]}\right) \sum_{r=1}^{n_{s+1}} e_{2_r}^{[s+1]} w_{rj}^{[s+1]} \tag{9}$$

Change of weight using (5), (6) and (7) for the selected neighborhood only.
Step 7. Weight updation
Update weights of output and hidden layer neurons using (10) for the selected neighborhood.

$$w_{ji}^{[s]}(t+1) = w_{ji}^{[s]}(t) + \Delta w_{ji}^{[s]} \tag{10}$$

Step 8. Repeat steps 3–7 for all the patterns.
Step 9. Evaluate network error with new weights.
Step 10. Stop learning process if terminating condition is reached.
Otherwise repeat the steps 2–10.

III. Features Extraction

As mentioned above, the main aim of our method is to diagnose diseases from a set of quantitative features that are extracted using image processing algorithms. There are three steps to get and extract the feature of the pancreatic texture in iris as follows: find iris boundaries, obtain region of interest (ROI) from pancreas location in iris, and do feature extraction.

A. Iris Localization

Iris is modeled by two circles, one for iris/pupil boundary and other for iris/sclera boundary and two parabolas for upper and lower eyelids. Daugman [11,12] built a recognition system using an integral-differential operator to find both the pupillary boundary and the outer (limbus) boundary of the iris (see Fig. 3). A very effective integral-differential operator for determining these parameters is:

$$\max_{(r,x_0,y_0)} \left| G_\sigma(r) * \frac{\partial}{\partial r} \oint_{r,x_0,y_0} \frac{I(x,y)}{2\pi r} ds \right| \tag{11}$$

where $I(x,y)$ is an image containing an eye. The operator searches over the image domain (x,y) for the maximum in the blurred partial derivative with respect to increase radius r, of the normalized contour integral of $I(x,y)$ along a circular arc ds of radius r and center coordinates (x_0,y_0). The symbol $*$ denotes convolution and $G_\sigma(r)$ is a smoothing function such as a Gaussian of scale σ. The complete operator behaves in effect as a circular edge detector, blurred at a scale set by σ, which searches iteratively for a maximum contour integral derivative with increasing radius at successively finer scales of analysis through the three parameters space of center coordinates and radius (x_0,y_0,r) defining a path of contour integration.

B. Obtaining Pancreas ROI

Based on Iridology chart [1], pancreas location in right eye of iris is in the third quarter of an eye ball at the position 06.45 – 07.15 with an estimated depth of 0.4 – 0.6 from the center of iris. The size of image taken from camera is 425x425 pixels, so the estimated size of the pancreas ROI is 32x32 pixels. The results of iris localization and obtaining ROI is shown in Fig. 3. below.

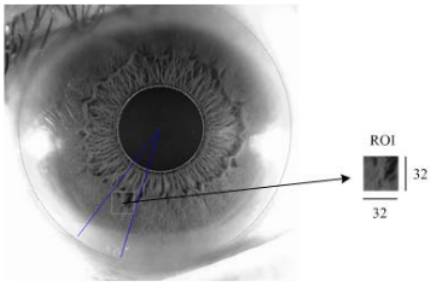

Fig. 3. Obtaining pancreas ROI in iris boundaries.

C. Quantitative Texture Features of Gray Level Co-occurrence Matrix

Gray Level Co-Occurrence Matrix (GLCM) can reveal certain properties about the spatial distribution of the gray levels in the texture image. For example, if most of the entries in the GLCM are concentrated along the diagonal, the texture is coarse with respect to the specified offset. However, a single direction of GLCM might not be enough to describe the textural features of the input image, so we used four directions GLCM with angle 0°, 45°, 90°, 135° and four distances of one pixel, two pixels, three pixels, and four pixels for each direction.

There are two feature-based texture operators, which are derived from the GLCM, are implemented to extract different textural features from ROI of iris. These two descriptors are the second moment, and contrast based on a GLCM, which are shown respectively as follows:

$$W_M = \sum_{g_1}\sum_{g_2} P^2(g_1, g_2) \tag{12}$$

$$W_C = \sum_{g_1}\sum_{g_2} |g_1 - g_2| P(g_1, g_2) \tag{13}$$

where $P(g_1, g_2)$ is a co-occurrence matrix, and g_1 and g_2 are two values of the gray level. W_M measures the smoothness or homogeneity of an image and it will reach its minimum value when all of the $P(g_1, g_2)$ have the same value. W_C is the first moment of the differences in the values of the gray level between the entries in the co-occurrence matrix. Thus, we obtain a set of textural features from ROI image which contains a total of 32 textural metrics as follows.

$$\begin{cases} TM_i = W_{M,i} & (i = 1,2,3,....,16), \\ TM_{i+16} = W_{C,i} \end{cases} \tag{14}$$

where $W_{M,i}$ and $W_{C,i}$ denote the measurements of and for each partition, respectively. To evaluate the performance of textural metrics in different directions and distances of the iris ROI, we introduce a new measurement, called grade of differentiation (GOD), which can be calculated as follows:

$$GOD_{M,i} = \left| \frac{\sum_{j=1}^{N} TM_{i,j}}{N} \right|; \; GOD_{C,i+16} = \left| \frac{\sum_{j=1}^{N} TM_{i+16,j}}{N} \right| \tag{15}$$

$$i = 1,2,3,...,16$$

where $GOD_{M,i}$ and $GOD_{C,i}$ are the mean of feature i from homogeneity and contrast for N data.

IV. Experimental Results

The experimental samples include 30 images from right iris affected by DM and 20 images from healthy volunteers. These samples were gathered using a specially designed eye camera called Dynolite Iriscope AMH-RUT and must meet inclusion and exclusion criteria to be obtained valid data. Inclusion criteria included subjects with type 1 and type 2 DM with fasting blood glucose over 200 mg/dL, perform at least 8 hours of fasting since the night until the time of blood taken, suspend the use of medications including insulin injections for at least 2 days until the time of blood taken, and signed informed consent. Whereas DM subjects exclusion criteria were subjects with less compliance. The inclusion criteria that must be met for healthy subjects are not experiencing polyuria, polydipsia, and polyfagia, blood glucose levels between 70, had no history of impaired glucose tolerance. Typical image of irises from patients with DM is shown in Fig. 4, together with an image of a normal iris for comparison.

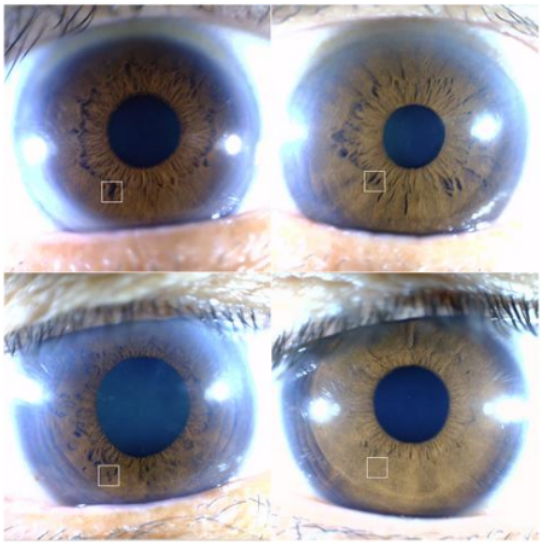

Fig. 4. Three iris image samples of patients suffering DM (upper left, upper right, lower left), and a typical normal iris image (lower right).

Validation results from a total of 30 right-eye images that are affected by DM, it is found out only 24 data can be used as test data. The six residual images cannot be used due to image blur, pancreas location covered by eyelids and there is a white ring that covers the location of the pancreas.

The results presented in this section are divided into four parts. The first part evaluates the location and position of broken tissue in iris by using real time image processing and compares the results with the analysis of Iridology practitioner. From 24 images with DM, the system can detect exactly 87.5% the presence of broken tissue (21 images are correct in detection and 3 images are false). So, for false location detection should be done manually.

The second part evaluates the performance of textural metrics using GOD. The results of feature extraction, we obtain a set of textual features which contains a total of 32 textural metrics as follows TM_1 up to TM_{32}. We try to eliminate the metrics which do not perform well for diagnosis of DM. Fig. 5 shows the results for the GODs of homogeneity. The best performing metrics are $GOD_{M,9}(90°,1)$, $GOD_{M,5}$ (45°,1), $GOD_{M,10}(90°,2)$, $GOD_{M,6}(45°,2)$, and $GOD_{M,11}$ (90°,3). Fig. 6 shows the results for the GODs of contrasts. A very interesting contrast can be seen for the $GOD_{C,30}$ (135°,2), $GOD_{C,29}$ (135°,1), $GOD_{C,18}$ (0°,2), $GOD_{C,24}$ (45°,4), and $GOD_{C,32}$ (135°,4). The diagnostic results of DM based on the 32 textural metrics and a subset, which is selected according to the performance presented in this section, of the total textural metrics are shown in Table I. It can be seen that, the average ratios of the correct classification are 2.4%, when using all textural metrics and rise up to 97.2%, when a subset of these metrics are used. Also, the values of false classification are decreased through this feature selection.

The third part evaluates the performance of ANMBP with different neighborhood sizes for $\alpha = 0.7$, $\lambda = 0.001$, maximum epochs = 500, and MSE = 0.001 then compares with BP result. The simulation results are compared and tabulated in Table II. Fig. 6 shows the learning curve based on epochs and MSE for ANMBP and BP. It can be seen that the ANMBP algorithm takes minimum number of time for convergence as compared with BP. It can also be observed that the adaptive learning rate becomes very small when the network gets trained, which is shown in Fig. 7.

The fourth part is to evaluate the diagnostic results of the algorithm ANMBP to determine the presence or absence of impaired pancreatic beta cell function and compare it with the calculated HOMA-B. HOMA-B is a method used to quantify insulin resistance and beta-cell function. HOMA-B calculation as follows:

$$HOMA - B(\%) = \frac{20\ x\ FastingInsulin(\mu U / ml)}{Bloodglu\cos e(mmol / l) - 3.5} \qquad (16)$$

Normal value of HOMA-B is in range 70-150. The diagnostic results are compared and tabulated in Table III. It can be seen that from the diagnostic results using ANMBP in 12 diabetic patients who have HOMA-B values below normal and have broken tissues, it is known that 10 patients can be detected correctly while the other two failed.

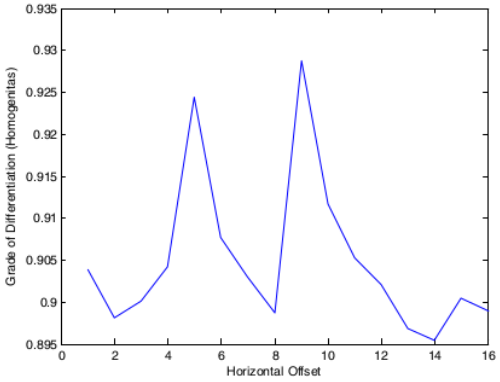

Fig. 4. GODs of the homogeneity.

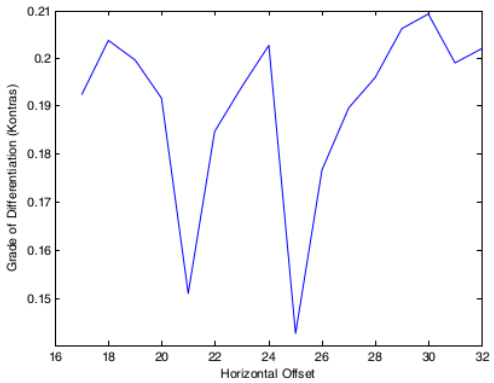

Fig. 5. GODs of the contrast.

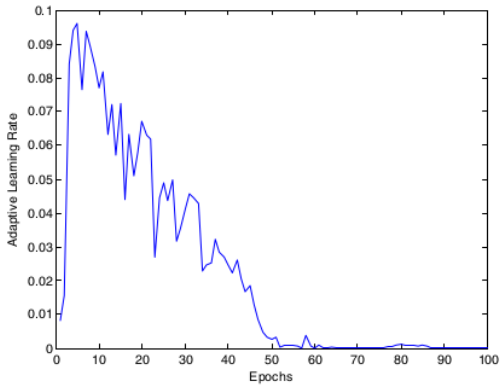

Fig. 6. Learning rate for the pancreatic disorders problem.

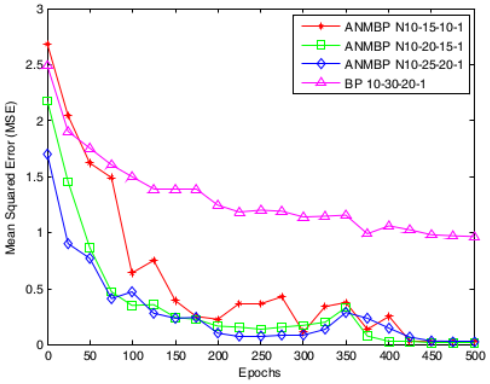

Fig. 7. Learning curve based on MSE and epochs of detecting pancreas condition for ANMBP and BP.

TABLE I
DIAGNOSTIC RESULTS OF PANCREATIC DISORDERS BY USING TEXTURAL METRICS

	TM1-TM32			TM5, TM6, TM9-TM11, TM18, TM24, TM29, TM30, TM32		
Simulation	(1)	(2)	(3)	(1)	(2)	(3)
Correct/Total	11/12	12/12	11/12	11/12	12/12	12/12
False/Total	1/6	1/6	0/6	0/6	0/6	0/6

TABLE II
COMPARISON TABLE OF ANMBP AND BP FOR PANCREATIC DISORDERS

Algorithm	Structure	Training MSE	Time in s
ANMBP	N10-15-10-1	0.008059	88.019516
	N10-20-15-1	0.007683	93.344066
	N10-25-20-1	0.006772	97.568455
BP	10-30-20-1	0.920442	219.963473

TABLE III
COMPARISON OF DIAGNOSTIC RESULTS OF ANMBP AND HOMA-B FOR DETECTION OF PANCREATIC DISORDERS

Patients	ANMBP N10-15-10-1	HOMA-B (%)
A	Broken Tissues	31.05
B	Broken Tissues	2.04
C	Broken Tissues	23.3
D	Broken Tissues	16.54
E	No Broken Tissues	67.17
F	Broken Tissues	10.23
G	Broken Tissues	24.33
H	Broken Tissues	37.83
I	Broken Tissues	48.25
J	No Broken Tissues	62.06
K	Broken Tissues	41.71
L	Broken Tissues	57.68

V. CONCLUSION

In this paper, we propose a computerized iris diagnosis method aimed at eliminating the subjective and qualitative characteristics of conventional iris diagnosis and establishing the relationship between iris appearance and the condition of pancreas organ. ANMBP classifiers based on quantative features namely textural measurements, is employed as the decision models for diagnosis. Experiments are carried out on a total of 30 in-patients affected by DM and 20 healthy volunteers.

Accuracy of determining the location of the pancreas in is is up to 87.5% after clarification by Iridology practitioner. The diagnostic results of DM by using a subset textural metrics provide a much better performance than those of whole textural metrics. ANMBP converged with minimum memory, weights and time compared with BP. Inclusion of adaptive learning parameters speeds up the convergence even for small neighborhood size and also the adapti learning rate becomes very small when networks get trained. The experimental results reasonably demonstrate the effectiveness of ANMBP method in comparison with HOMA-B can achieve an accuracy of 83.3% in detecting pancreatic disorders. Compared with the isting approaches, the method presented in this paper es blishes a mapping from quantitative features to diseases, so it could expedite its use in clinical applications.

REFERENCES

[1] Jensen, B., (1980), Iridology Simplified – An Introduction to the Science of Iridology and its Relation to Nutrition, Iridologists International Route 1, Box 52, Escondido, California 92025, U.S.A.

[2] A. D. Wibawa and M. H. Purnomo, "Early Detection on the Condition of Pancreas Organ as the Cause of Diabetes Mellitus by Real Time Iris Image Processing," APCCAS Circuits and Systems, 2006, pp. 1008-1010.

[3] Lin Ma and Naimin Li, "Texture Feature Extraction and Classification for Iris Diagnosis," ICMB, LNCS 4901, 2007, pp.168-175.

[4] R. A. Ramlee and S. Ranjit, "Using Iris Recognition Algorithm, Detecting Cholesterol Presence," ICIME Information Management and Engineering, Kuala Lumpur, Malaysia, 2009.

[5] S. Abid, F. Fnaiech, and M. Najim, "A Fast Feedforward Training Algorithm using A Modified Form of the Standard Backpropagation Algorithm," IEEE Trans. Neural Networks 12, 2001, pp. 424–430.

[6] G. Lera and M. Pinzolas, "Neighborhood based Levenberg–Marquardt Algorithm for Neural Network Training," IEEE Trans. Neural Networks 13, 2002, pp. 1200–1204.

[7] L. Behera, S. Kumar, and A. Patnaik, "On Adaptive Learning Rate that Guarantees Convergence in Feedforward Networks," IEEE Trans. Neural Networks 17, 2006, pp. 1116–1125.

[8] T. Kathirvalavakumar and S. J. Subavathi, "Neighborhood based Modified Backpropagation Algorithm using Adaptive Learning Parameters for Training Feedforward Neural Networks," Neurocomputing 72, 2009, pp. 3915-3921.

[9] W. Wei, F. Guorui, L. Zhengxue, and X. Yuesheng, "Deterministic Convergence of An Online Gradient Method for BP Neural Network," IEEE Trans. Neural Networks 16, 2005, pp. 533–540.

[10] X. Yu, M. O. Efe, and O. Kaynak, "A General Backpropagation Algorithm for Feedforward Neural Networks Learning," IEEE Trans. Neural Networks 13, 2002, pp. 251–259.

[11] J. G. Daugman, "High Confidence Visual Recognition of Persons by A Test of Statistical Independence," IEEE Trans. on Pattern Analysis and Machine Intelligence, vol. 15, no. 11, 1993, U.S.A, pp. 1148–1161.

[12] J. G. Daugman, "How Iris Recognition Works," IEEE Trans. on Circuits and Systems for Video Technology, vol. 14, no. 1, 2004, pp. 21-30.

Paper Jurnal/Prosiding

ORIGINALITY REPORT

22%	18%	27%	12%
SIMILARITY INDEX	INTERNET SOURCES	PUBLICATIONS	STUDENT PAPERS

PRIMARY SOURCES

1	G. Lera, M. Pinzolas. "Neighborhood based Levenberg-Marquardt algorithm for neural network training", IEEE Transactions on Neural Networks, 2002 Publication	5%
2	David Zhang, Hongzhi Zhang, Bob Zhang. "Chapter 15 Tongue Image Analysis for Appendicitis Diagnosis", Springer Science and Business Media LLC, 2017 Publication	4%
3	www.scribd.com Internet Source	3%
4	www.pragyan.org Internet Source	3%
5	namanmaheshwari.in Internet Source	3%
6	Zhang, David, Wangmeng Zuo, and Naimin Li. "Computerized Tongue Diagnosis", Medical Biometrics, 2016. Publication	2%

7	ebin.pub Internet Source	2%

Exclude quotes	On	Exclude matches	< 2%
Exclude bibliography	On		